HHS Public Access

Author manuscript

Addict Biol. Author manuscript; available in PMC 2017 July 01.

Published in final edited form as:

Addict Biol. 2016 July ; 21(4): 939–953. doi:10.1111/adb.12232.

Diffusion Tensor Imaging Reveals Adolescent Binge Ethanol-induced Brain Structural Integrity Alterations in Adult Rats that Correlate with Behavioral Dysfunction

Ryan P. Vetreno, **Richard Yaxley**, **Beatriz Paniagua**, and **Fulton T. Crews**

The Bowles Center for Alcohol Studies, Department of Psychiatry, The University of North Carolina at Chapel Hill, Chapel Hill, NC 27599 USA

Abstract

Adolescence is characterized by considerable brain maturation that coincides with the development of adult behavior. Binge drinking is common during adolescence, and can have deleterious effects on brain maturation due to the heightened neuroplasticity of the adolescent brain. Using an animal model of adolescent intermittent ethanol (AIE; 5.0 g/kg, i.g., 20% EtOH w/v; 2 days on/2 days off from postnatal day [P]25 to P55), we assessed adult brain structural volumes and integrity on P80 and P220 using diffusion tensor imaging (DTI). While we did not observe a long-term effect of AIE on structural volumes, AIE did reduce axial diffusivity (AD) in the cerebellum, hippocampus, and neocortex. Radial diffusivity (RD) was reduced in the hippocampus and neocortex of AIE-treated animals. Prior AIE treatment did not affect fractional anisotropy (FA), but did lead to long-term reductions of mean diffusivity (MD) in both the cerebellum and corpus callosum. Adolescent intermittent ethanol resulted in increased anxiety-like behavior and diminished object recognition memory, the latter of which was positively correlated with DTI measures. Across aging, whole brain volumes increased, as did volumes of the corpus callosum and neocortex. This was accompanied by age-associated AD reductions in the cerebellum and neocortex as well as RD and MD reductions in the cerebellum. Further, we found that FA increased in both the cerebellum and corpus callosum as rats aged from P80 to P220. Thus, both age and AIE treatment caused long-term changes to brain structural integrity that could contribute to cognitive dysfunction.

Keywords

Adolescence; alcohol; development; memory; binge drinking

Corresponding author: Ryan P. Vetreno, Ph.D., University of North Carolina at Chapel Hill, School of Medicine, Bowles Center for Alcohol Studies, CB #7178, 1021 Thurston-Bowles Building, Chapel Hill, NC 27599-7178, Tel: 1-919-966-0501, Fax: 1-919-966-5679, rvetreno@email.unc.edu.

Author Contributions

RPV and FTC were responsible for the study concept and design. All authors contributed equally to the data preparation and analyses. RPV drafted the manuscript. RPV, RY, BP, and FTC were involved in editing and have approved the final version for publication.

Introduction

Human neuroimaging studies find that adolescent maturation of grey and white matter structures supports the transition of the immature child brain to the mature networks that characterize the adult brain (Giedd, 2004). Unfortunately, adolescence is also a time when individuals initiate alcohol use and abuse (Spear, 2011) as 5% of 8th grade, 14% of 10th grade, and 22% of 12th grade individuals report heavy episodic drinking (i.e., >5 consecutive alcohol drinks per episode) over the past two weeks (Johnston et al., 2013). This heavy drinking pattern continues through college as 41% of male students report binge drinking every 2 weeks while 8% report consuming ≥ 3 times the binge threshold during a 2-week period (White et al., 2006). Routine binge drinking might lead to long-term changes in adult neurobiology due to the heightened neural plasticity and structural development that characterizes the adolescent brain (Crews et al., 2007). An earlier age of drinking onset (i.e., 11 – 14 years of age) increases the risk of developing an alcohol use disorder later in life (DeWit et al., 2000). Further, adolescent binge drinking is associated with diminished impulse inhibition (White et al., 2011), reduced attentional functioning (Koskinen et al., 2011), deficits in visuospatial ability (Tapert et al., 2002), and impaired executive functioning (White et al., 2011). These findings support the hypothesis that adolescent binge drinking alters neuromaturational processes that culminate in long-term behavioral changes.

Over the past decade, non-invasive neuroimaging technologies have been used to elucidate the neuroarchitectural changes associated with adolescent binge drinking. Magnetic resonance imaging (MRI) studies of adolescent binge drinkers reveal altered structural volumes in several brain regions, including the hippocampus, prefrontal cortex, and cerebellum (for review, see Welch et al., 2013). Diffusion MRI, also known as diffusion tensor imaging (DTI), provides a measure of grey and white matter integrity by assessing the magnitude and orientation of water molecule diffusion in the brain (Oguz et al., 2012). During adolescent brain development, white matter structures mature hierarchically and become highly organized, which is concomitant with maturation of cognitive faculties (Bava and Tapert, 2010; Lenroot and Giedd, 2006). Several DTI studies have reported altered diffusivity measures in white matter structures of human binge drinkers (Jacobus et al., 2009; McQueeny et al., 2009), but these data are difficult to interpret as it is unknown whether alcohol exposure or a pre-existing condition led to heavy binge drinking, and the subsequent brain and behavioral changes. Thus, animal neuroimaging studies provide a useful tool for directly assessing the effects of alcohol on the developing brain because they allow for the systematic control of extraneous variables.

Similar to human studies, animal models of adolescent binge drinking find ethanol-induced alterations of brain structural volumes (Coleman et al., 2011; Ehlers et al., 2013). For instance, Ehlers and colleagues (2013) found adolescent maturational changes in hippocampal volumes of young adult rats following adolescent binge ethanol exposure, which was correlated with measures of anxiety-like behavior. However, the effect of adolescent binge ethanol exposure on the structural integrity of grey and white matter regions is unknown. In this study, DTI was used to test the hypothesis that adolescent intermittent ethanol (AIE) treatment of male Wistar rats leads to long-term alterations in grey and white matter integrity from P80 to P220. From the DTI, we assessed four scalar

variables: mean diffusivity (MD), the overall magnitude of water diffusion; fractional anisotropy (FA), a measure of the directional coherence of water diffusion; axial diffusivity (AD), the magnitude of water diffusion parallel to axons; and radial diffusivity (RD), the magnitude of water diffusion perpendicular to the axon. Fractional anisotropy is related to increased axon density and/or myelination (Beaulieu, 2002), but alone will not help to explain the nature of the white matter microstructure. Therefore, both AD and RD were also investigated. These studies provide insight into the impact of adolescent binge drinking models and age on adult brain structure.

Materials and Methods

Animals

Young pregnant female Wistar rats (embryonic day 17; Harlan Sprague-Dawley, Indianapolis, IN) were acclimated to our animal facility prior to birthing at the University of North Carolina at Chapel Hill. On P1 (24 hr after birth), litters were culled to 10 pups and. housed with their mother until group housing with same-sex littermates at the time of weaning on P21. All animals were housed in a temperature- (20°C) and humidity-controlled vivarium on a 12 hr/12 hr light/dark cycle (light onset at 0700 hr), and provided *ad libitum* access to food and water. Experimental procedures were approved by the IACUC of the University of North Carolina at Chapel Hill, and conducted in accordance with NIH regulations for the care and use of animals.

Adolescent Intermittent Ethanol Treatment Paradigm

On P21, male Wistar rats (N = 32) were weaned, group housed (n = 4 per cage), and randomly assigned to either (i) adolescent intermittent ethanol (AIE; n = 16) or (ii) water-treated control (CON; n = 16). Subjects were further divided into the P80 (CON = 8 and AIE= 8) and P220 (CON = 8 and AIE= 8) age groups. Beginning on P25, AIE-treated animals received intragastric (i.g.) administration of ethanol (5.0 g/kg, 20% ethanol w/v) on a 2-day on/2-day off schedule until P55. Animals in the CON condition received comparable volumes of H_2O on the same schedule. As seen in Fig. 1, all subjects gained weight during the course of experimentation. There was no difference in body weight (mean ± S.D.) during AIE treatment ($p > 0.4$) as all subjects grew from 73 (±10) g on P25 to 301 (±28) g on P57, with CONs weighting 311 (±27) g and AIEs weighing 291 (±27) g. Body weight did not differ as a function of treatment at the time of sacrifice in the P80 group ($p > 0.2$), but did differ at the time of sacrifice in the P220 group ($p < 0.05$).

Blood samples were collected from the tail on P38 and P54 and blood ethanol content (BECs) was analyzed using a GM7 Analyzer (Analox; London, UK). Mean BEC levels (mean ± S.D.) on P38 were 168 (±47) mg/dL and at P54 were 178 (±66) mg/dL, which are consistent with previous studies from our laboratory (Vetreno and Crews, 2012). Following the conclusion of AIE treatment, subjects were housed in pairs (n = 2 per cage), and maintained on *ad libitum* access to food and water for the duration of the experiments. Prior to behavioral testing, subjects were only handled during treatment and weighing sessions.

Behavioral Assessment: Open-field Object Recognition Memory

Object recognition memory was assessed from P163 to P165 using an open-field apparatus (65 cm × 65 cm × 47 cm), which was constructed of wood and painted black. The testing environment was brightly illuminated by four 100 watt lights suspended above the apparatus and white noise provided by a white noise generator. An automated tracking system (Ethovision XT 8.0, Noldus Ethovision; Leesburg, VA) was used to monitor behavior, and between each trial the open-field and each object was thoroughly cleansed (Roccal-D Plus, Fisher Scientific; Pittsburgh, PA) to remove all olfactory cues. Before each trial, subjects were habituated to the testing environment for 10 min. On the first day of testing (habituation phase), individual rats were placed on the open-field in the bottom right facing the corner. The subject was allowed to freely explore the open-field for 5 min, and distance traveled (cm), latency to enter the center (s), and duration (s) and entries into the center were recorded. Twenty-four hrs later during the familiarization phase (Trial 2), two texturally and visually different objects (glass Mason jar [A] and plastic bottle [B]) were placed in opposite corners in the middle of the open-field apparatus. The subject was allowed to freely explore the open-field and objects for 5 min. Duration (s) and number of contacts with each object was quantified as was the distance traveled (cm). Twenty-four hrs later on the third day of testing (testing phase), Object B was replaced with novel Object C (ceramic mug), and the duration (s) and number of contacts with the familiar (F) and novel (N) object was quantified as was the distance traveled (cm). A contact was defined as the subject directing the nose <2 cm from the object, or directly touching it. The discrimination ratio, which provides a measure of novel object exploration (Antunes and Biala, 2012; Bartolini et al., 1996), was calculated by: (Novel − Familiar)/(Novel + Familiar). The discrimination ratio varies between +1 and −1, with a positive ratio signifying more time spent exploring the novel object while a negative ratio reflects more time spent with the familiar object. A ratio of 0 indicates that equal time was spent exploring both objects (Antunes and Biala, 2012).

Behavioral Assessment: Behavior in the Light/Dark Box

On P219, anxiety-like behavior was assessed in the light/dark box (68 cm × 21 cm × 36 cm; San Diego Instruments, San Diego, CA) and was divided into two equal chambers (34 cm × 21 cm × 36 cm). The dark box was opaque while the light box was brightly illuminated with a chamber light that was positioned 36 cm above the base. An opaque divider separated the light and dark boxes with a small opening at the base that allowed passage of the animal between chambers. An automated tracking system (Photobeam Activity System, San Diego Instruments), consisting of infrared photocell beams placed 2 cm above the floor, was used to track each subjects movement. On the day of testing, each rat was individually transported to the testing room, which was dark and filled with white noise, and habituated to the testing environment for 10 min. Following habituation, each subject was placed into the center of the dark box and allowed to freely explore the apparatus for 5 min. Latency to enter the light box (s), entries into the light box, and duration in the light box (s) was measured throughout the session. Between each subject, the apparatus was thoroughly cleansed to remove all olfactory cues.

Tissue Perfusion for Neuroimaging

On P80 and P220, subjects were anesthetized with an overdose of sodium pentobarbital (100 mg/kg, i.p.). Animals were transcardially perfused at a flow rate of 30 mL/min on a heating pad with a 1:10 solution of ProHance® (Bracco Diagnositics, Princeton, NJ) in 0.9% saline at 37°C, followed by 1:10 solution of ProHance® in 10% formalin (pH 7.4) at room temperature (Oguz et al., 2013). ProHance is a contrast agent that improves scan resolution. The skull with brain intact was stored in a specimen container in a 10% formalin solution at 4 ° C. Twenty-four hr later, the skull with brain intact was transferred to a 1:100 solution of ProHance® in phosphate-buffered saline (PBS, pH 7.4) at 4 °C until the DTI session.

DTI Acquisition

A total of 32 rat skulls with brain intact were sent to the University of North Carolina at Chapel Hill Biomedical Research Imaging Center (BRIC) for DTI in a dedicated 9.4T Bruker small animal scanner. The acquisition of DTI enabled the analysis of structural volume and diffusion data. Diffusion tensor images were acquired with isotropic voxels (0.16 mm × 0.16 mm × 0.16 mm) were acquired using a diffusion-weighted 3D RARE sequence with 12 quasi-uniformly distributed diffusion encoding gradient directions and 3 baseline images. The total scan time was approximately 15 hrs per subject. Although acquiring a higher number of diffusion directions would have increased the accuracy of the DTI measurement computation, we decided against acquiring a higher number of diffusion directions (e.g., 20) as it would have significantly impacted spatial resolution or the Signal-to-Noise ratio (SNR). Further, we wanted to maintain consistency in reported methods in the recently published atlas manuscripts (Calabrese et al., 2013; Chuang et al., 2011).

Image Processing

The DTI data was processed using our fully automatic pipeline (Budin et al., 2013) with thorough quality control checks after each step. After the raw data were bias corrected, diffusion tensors were estimated and diffusion property maps, including AD, RD, MD, and FA, were computed for each subject (see Fig. 2A). These images were rigidly aligned (translation and rotation) with a pre-existing atlas (Rumple et al., 2013) using mutual information. The entire diffusion tensor field was transformed using these rigid transforms according to Log-Euclidean interpolation (Arsigny et al., 2006) and the diffusion property maps were recomputed in this atlas space.

The rigidly registered MD images were used for skull stripping the images using an atlas-based tissue classification method (see Oguz et al., 2011). The skull stripped images were deformably co-registered in a group-wise manner to compute an unbiased population average (Joshi et al., 2004). The pre-existing atlas was registered to the population average, and the accompanying segmentation into 7 regions of interest (ROI), which included the amygdala, cerebellum, corpus callosum, hippocampus, hypothalamus, neocortex, and striatum) were propagated along these computed deformation fields, first to the population average and then to the individual subjects. Of these regions, we focused our analyses on the cerebellum, corpus callosum, hippocampus, and neocortex (see Fig. 2B) as these brain regions are typically reported as vulnerable to the effects of alcoholism in the human literature (De Bellis et al., 2000; De Bellis et al., 2005; Lisdahl et al., 2013; McQueeny et

al., 2009). Rigorous quality control was performed after each step to ensure automatic processing performance was satisfactory.

The prolonged postmortem scan allows the acquisition of isotropic DTI data with a high resolution both in-plane and out-of-plane. Therefore, we were able to align and segment the images in 3D and compute the volume of each structure in each subject. Additionally, the atlas-based segmentation of the entire brain at once allowed for smooth and accurate boundaries between neighboring regions, compared to a region-by-region basis that may have biased the analysis based on the order of processing.

Statistical Analysis

The Statistical Package for the Social Sciences (SPSS; Chicago, IL) was used for all statistical analyses. The effect of AIE on body weight was assessed using a repeated measures ANOVA. One-way ANOVAs were used to assess BECs and all behavioral data. Independent ANOVAs (AGE [P80 vs. P220] × TREATMENT [CON vs. AIE]) were used to assess the effect of AIE on volume and diffusivity measures. DTI data was also analyzed with independent sample t-tests to determine the effects of AIE on volume and diffusivity measures in each age group. Since performing multiple comparisons can increase the incidence of Type I Errors, the Benjamini-Hochberg procedure (B-H Critical) for controlling false positives was calculated (Thissen et al., 2002). Although the experiment began with 8 subjects per group, several subjects were lost due to technical issues during DTI scanning procedure. Consequently, there were a total of 5 subjects per treatment in the P80 age group and 7 subjects per treatment in the P220 age group for the imaging studies. Pearson correlations (r) were used to assess the association between brain volumes (mm^3) obtained from DTI with wet brain volumes (g) as well as correlations between behavioral measures and the structural diffusivity data. All values are reported as mean ± SEM, and significance was defined at a level of $p \leq 0.05$.

Results

Structural analysis reveal increased overall brain and discrete brain regional growth with age

To model human adolescent drinking behavior, we used an intermittent schedule consistent with known patterns of heavy weekend drinking, but not daily drinking associated with adult alcoholism. To determine the effects of aging and AIE on brain morphology, we used structural DTI to assess volumes of the whole brain as well as brain regions predicted to change in P80 and P220 CON- and AIE-treated rats. Analysis of total brain volume revealed a significant 10% (±1%) increase from P80 to P220 (see Fig. 3A). To determine the association of the total brain volume with physiological measures, we correlated total brain volume (cm^3) with wet brain weight (g). As depicted in Fig. 3B, total brain volume was positively correlated with wet brain weight. Brain regional volume analysis found two brain regions to be increased significantly with age. The corpus callosum increased by 28% (±3%) from P80 to 220 (see Fig. 4A) and. the volume of the neocortex increased by 13% (±1%) from P80 to P220 (see Fig. 4B). No other main effects or interactions were observed in the other brain regional volumes assessed (see Table 1). Together, these data reveal an age-

associated increase in whole brain, neocortical grey matter, and corpus callosum white matter volumes from P80 to P220.

Diffusion tensor imaging reveals that AIE and aging affect measures of water diffusivity

Diffusion tensor imaging allows for non-invasive assessment of grey and white matter structural integrity by measuring the magnitude and direction of water diffusion. Across age, we found that AD was reduced by 20% (±2%) in the cerebellum. We found a similar age-associated 11% (±2%) reduction of AD in the neocortex from P80 to P220. In addition, AD was reduced by 18% (±2%) in the amygdala (main effect of AGE: $F_{(1,20)} = 5.5$, $p < 0.05$) and by 27% (±2%) in the hypothalamus (main effect of AGE: $F_{(1,20)} = 9.7$, $p < 0.01$) from P80 to P220. Analysis of the cerebellum revealed an AIE-induced 15% (±4%) reduction of AD in adult rats, relative to CONs. Within the hippocampus, AD was also reduced by 11% (±1%) in the AIE-treated adult animals, relative to the CONs. Further, analysis of the neocortex also revealed a significant 12% (±2%) reduction of AD in the AIE-treated animals, relative to the CONs (see Fig. 5). There were no other main effects or interactions with AIE treatment (see Table 2). These data reveal that AD undergoes region specific age-associated decline from P80 to P220 while it is decreased in the adult cerebellum, hippocampus, and neocortex following AIE treatment.

From P80 to P220, RD was reduced by 25% (±2%) in the cerebellum. Further, RD was reduced by 22% (±2%) in the amygdala (main effect of AGE: $F_{(1,20)} = 6.7$, $p < 0.05$) and 35% (±3%) in the hypothalamus (main effect of AGE: $F_{(1,20)} = 11.9$, $p < 0.01$) from P80 to P220. In the hippocampus, RD was reduced by 11% (±2%) in adult animals following AIE treatment. Radial diffusivity was also reduced by 12% (±2%) in the neocortex of AIE-treated adult animals, relative to the CONs (see Fig. 6). There were no other main effects or interactions with AIE treatment (see Table 3). Together, these data reveal region specific decreases in RD with age from P80 to P220, and that AIE treatment leads to long-term reductions of RD in the hippocampus and neocortex.

Mean diffusivity declined by 10% (±2%) in the cerebellum from P80 to P220. Similarly, MD was reduced by 17% (±3%) in the hypothalamus of P220 animals when compared to the P80 animals (main effect of AGE: $F_{(1,20)} = 17.3$, $p < 0.01$). Adolescent intermittent ethanol resulted in a significant by 17% (±3%) reduction of MD in the adult cerebellum, relative to the CONs. We also found that AIE treatment resulted in a similar 10% (±2%) reduction of MD in the corpus callosum of adult rats, relative to CONs (see Fig. 7). There were no other main effects or interactions for MD (see Table 4). These data reveal brain regional specific reductions of MD from P80 to P220, and that MD was reduced by AIE treatment in the adult cerebellum and corpus callosum.

Fractional anisotropy was significantly increased by 13% (±2%) in the cerebellum from P80 to P220. Similarly, there was a significant 37% (±3%) increase in FA in the corpus callosum from P80 to P220 (see Fig. 8). Further, FA was increased in the hypothalamus from P80 to P220. There were no other main effects or interactions (see Table 5). Together, these data reveal an age-associated increase in FA in the cerebellum, corpus callosum, and hypothalamus from P80 to P220.

Object recognition memory is impaired in adult rats following AIE treatment

Previous studies found that adolescent binge ethanol treatment of mice reduces object recognition 3 weeks after ethanol treatment (Pascual et al., 2007). We used the open-field novel object recognition task to assess object recognition memory from P163 to P165 in adult rats following adolescent binge ethanol treatment. During the habituation phase, AIE-treated animals evidenced greater latencies to enter the center of the apparatus, relative to CONs (see Fig. 9A). There was no effect of AIE treatment on distance traveled, duration in the center, or number of entries into the center (all p's > 0.08). Adolescent binge ethanol exposure did not affect any of the measures during the familiarization phase (all p's > 0.1). During the testing phase, AIE treatment significantly reduced the discrimination ratio relative to CONs (see Fig. 9B). Together, these data reveal that AIE treatment leads to long-term impairments of object recognition memory and increased the latency to enter the center of the maze.

Adolescent intermittent ethanol treatment leads to long-term anxiety-like behavior in adult rats

Given our finding of AIE-induced thigmotaxis on the object recognition task, we assessed anxiety-like behavior on P219 using the light/dark box. Time spent in the light box was reduced by 30% (±7%) in the AIE-treated animals, relative to the CONs (see Fig. 10). There was no difference in latency or number of entries into the light box (both p's > 0.5). Thus, these data, coupled with the increase in thigmotaxis, reveal that AIE treatment leads to long-term increases in anxiety-like behavior.

Diffusion tensor measures of AD correlate with object recognition memory performance in adulthood

Brain structures and white matter tracts that support the integration of executive and emotive function continue to mature through adolescence into adulthood (Wu et al., 2014). We sought to determine whether there was a relationship between DTI measures and performance on the object recognition memory task and light/dark box. Diffusion measures correlated with object recognition memory as assessed with the discrimination index (see Table 6). Object recognition memory was positively correlated with AD in the neocortex, hippocampus, and cerebellum. A comparison of AD in each of these brain regions with the discrimination index reveals that lower AD measures were associated with diminished performance on the object recognition task (see Fig. 11). Performance on the light/dark box did not correlate with DTI measures (data not shown). These correlations are consistent with altered axonal integrity contributing to the cognitive impairments associated with adolescent binge ethanol exposure.

Discussion

This is the first experiment to use DTI to assess the effect of AIE treatment on the structural integrity of the aging rat brain. We tested the hypothesis that AIE leads to long-term structural alterations in grey and white matter integrity that may be related to altered cognitive processes in adulthood. While AIE exposure did not affect structural volumes, we did find AIE-induced reductions of AD in the cerebellum, hippocampus, and neocortex.

Further, RD was reduced in the hippocampus and neocortex of AIE-treated animals. Prior AIE treatment did not affect measures of FA, but did lead to long-term reductions of MD in both the cerebellum and corpus callosum. Across age groups, whole brain volume increased, as did corpus callosum and neocortex volumes from P80 to P220. These increased volumes were accompanied by age-associated AD reductions in the cerebellum and neocortex as well as RD and MD reductions in the cerebellum. Further, we found that FA increased in both the cerebellum and corpus callosum as rats aged from P80 to P220. Behaviorally, AIE treatment resulted in increased anxiety-like behavior and diminished object recognition memory, the latter of which was positively correlated with DTI measures. Taken together, these data reveal that AIE treatment leads to long-term alterations of structural integrity in brain regions critically involved in cognitive processes that might contribute to the behavioral dysfunction observed in adulthood.

Human neuroimaging studies provide considerable evidence of brain regional volume deficits in adult alcoholics (see e.g., Pfefferbaum et al., 1996). Similar morphological changes have been observed in the brains of adolescent binge drinkers (De Bellis et al., 2000; Lisdahl et al., 2013). However, there is considerable variation in the adolescent findings, which is likely a consequence of both differences in brain maturation across individuals and varied statistical power to identify small differences. For instance, Lisdahl and colleagues (2013) found that heavy alcohol use during adolescence reduced volumes of the cerebellum as measured using MRI while others report that cerebellar volumes were unaffected (De Bellis et al., 2005). In the present study, we focused our assessment on major brain regions that undergo maturational changes during adolescence. Our volumetric DTI analysis did not reveal an effect of AIE treatment on overall or brain regional volumes in adulthood. Similarly, Ehlers and colleagues (2013) found that AIE treatment did not affect volumes of the total brain or corpus callosum. However, they did report an interaction of age by treatment in the hippocampus. Our lack of an AIE effect on hippocampal volumes in the present study might be due to the loss of statistical power associated with the small sample size. Thus, our AIE model does not lead to statistically significant long-term alterations in adult brain regional volumes.

The advent of DTI, which allows for inferences of structural integrity by measuring the magnitude and directionality of water movement, provides further insight into the effects of AIE on brain morphology. The majority of human adolescent studies focused on white matter tracts, often reporting that increased alcohol consumption is associated with altered white matter integrity (McQueeny et al., 2009). Our finding of AIE-induced reductions of AD in the neocortex, hippocampus, and cerebellum of adult rats is indicative of axonal injury and/or reduced axonal density (Mac Donald et al., 2007; Song et al., 2003), which might contribute to cognitive dysfunction. Further, RD was decreased in the hippocampus and neocortex of AIE-treated adult rats, which might be attributable to increased tissue density in these gray matter structures. Indeed, extracellular matrix (ECM) proteins, which are a complex network of neurophil that aggregate to form perineuronal nets, are increased in the adult brain following AIE treatment (Coleman et al., 2014). Ethanol exposure leads to ECM reorganization and/or deposition (Wright et al., 2003) that could increase tissue density resulting in diminished RD values in the AIE-treated adult animals. We also found reduced MD values in the cerebellum and corpus callosum of AIE-treated animals. Lower

MD values are associated with increased tissue density (Roberts and Schwartz, 2007). Consistent with our findings, De Bellis and colleagues (2008) found increased FA and decreased MD values in the corpus callosum of adolescent binge drinkers, indicative of accelerated myelination relative to age-matched controls. Together, these data reveal that adolescent binge ethanol exposure leads to long-term alterations to brain regional anisotropy.

During adolescence, the brain undergoes significant refinement that parallels the attainment of adult cognitive processes (Ernst et al., 2009). Heavy patterns of binge drinking might lead to long-term changes in adult neurobiology due to the heightened neural plasticity and structural development that characterizes the adolescent brain (Crews et al., 2007). We found long-term object recognition memory impairments and increased anxiety-like behavior in adult rats following AIE treatment. These findings are consistent with data from our laboratory (Coleman et al., 2011; Vetreno and Crews, 2012) and others (Ehlers et al., 2013) of cognitive and emotive dysfunction in young adult rats and mice following AIE treatment. In humans, adolescent binge drinking is also associated with diminished attentional and executive functioning (Koskinen et al., 2011; White et al., 2011). Although anxiety-like behavior did not correlate with measures of diffusivity, object recognition memory impairments were correlated with structural integrity, particularly in the neocortex, hippocampus, and cerebellum. This is consistent with the emerging interactions of the neocortex with the cerebellum (Jung et al., 2014) as well as the role of the hippocampus (Squire, 1992), in learning and memory. For instance, Jung and colleagues (2014) found that cognitive dysfunction in recovering human alcoholics is associated with compromised cortical-cerebellar circuitry. Thus, alterations in axonal and structural integrity might contribute to cognitive dysfunction due to dysregulation of pruning processes necessary to refine the circuitry and remove redundant signaling pathways. Clearly, further research is necessary to fully investigate this finding as it relates to altered cognitive processes.

Diffusion tensor imaging allows for the elucidation of the maturational brain changes that occur during adolescence. In rats, developmental increases in total brain volume and regional volumes are observed from P28 to P80 (Oguz et al., 2013). Interestingly, in the present study we found that total brain volume, neocortical grey matter, and corpus callosum white matter volumes continue to increase through adulthood. We also observed age-associated FA increases and MD reductions in the corpus callosum and cerebellum, suggesting that structural refinement might also continue into adulthood. In the human adolescent brain, DTI revealed FA increases and MD decreases in white matter structures, which is consistent with increased myelination (Wang et al., 2012). Indeed, FA increases and MD decreases from early adolescence to early adulthood were observed in the corpus callosum and cerebellum of the rhesus monkey (Shi et al., 2013).

In summary, aging and adolescent binge ethanol treatment led to long-term changes in the structural integrity of brain structures critically involved in cognitive processes. Further, AIE treatment led to long-term memory deficits and increased anxiety-like behavior in adults. The memory deficits on the object recognition task were positively correlated with DTI measures supporting our hypothesis that AIE induces maturational changes to the brain that persist into adulthood and contribute to neurocognitive dysfunction. Together, these data are

consistent with underage binge drinking producing long lasting morphological changes in the developing CNS that impact adult neurocognitive function.

Acknowledgments

This work was supported in part by the National Institutes of Health, National Institute on Alcoholism and Alcohol Abuse (AA019767, AA11605, AA007573, and AA021040), the Neurobiology of Adolescent Drinking in Adulthood (NADIA [AA020023, AA020024, and AA020022]), and the Bowles Center for Alcohol Studies. The authors thank Diana Lotito for help with preparation of the manuscript.

References

ANTUNES M, BIALA G. The novel object recognition memory: neurobiology, test procedure, and its modifications. Cognitive processing. 2012; 13:93–110. [PubMed: 22160349]

ARSIGNY V, FILLARD P, PENNEC X, AYACHE N. Log-Euclidean metrics for fast and simple calculus on diffusion tensors. Magn Reson Med. 2006; 56:411–421. [PubMed: 16788917]

BARTOLINI L, CASAMENTI F, PEPEU G. Aniracetam restores object recognition impaired by age, scopolamine, and nucleus basalis lesions. Pharmacology, biochemistry, and behavior. 1996; 53:277–283.

BAVA S, TAPERT SF. Adolescent brain development and the risk for alcohol and other drug problems. Neuropsychology review. 2010; 20:398–413. [PubMed: 20953990]

BEAULIEU C. The basis of anisotropic water diffusion in the nervous system - a technical review. NMR in biomedicine. 2002; 15:435–455. [PubMed: 12489094]

BUDIN F, HOOGSTOEL M, REYNOLDS P, GRAUER M, O'LEARY-MOORE SK, OGUZ I. Fully automated rodent brain MR image processing pipeline on a Midas server: from acquired images to region-based statistics. Frontiers in neuroinformatics. 2013; 7:15. [PubMed: 23964234]

CALABRESE E, BADEA A, WATSON C, JOHNSON GA. A quantitative magnetic resonance histology atlas of postnatal rat brain development with regional estimates of growth and variability. NeuroImage. 2013; 71:196–206. [PubMed: 23353030]

CERCIGNANI M, INGLESE M, PAGANI E, COMI G, FILIPPI M. Mean diffusivity and fractional anisotropy histograms of patients with multiple sclerosis. AJNR American journal of neuroradiology. 2001; 22:952–958. [PubMed: 11337342]

CHUANG N, MORI S, YAMAMOTO A, JIANG H, YE X, XU X, RICHARDS LJ, NATHANS J, MILLER MI, TOGA AW, SIDMAN RL, ZHANG J. An MRI-based atlas and database of the developing mouse brain. NeuroImage. 2011; 54:80–89. [PubMed: 20656042]

COLEMAN LG JR, HE J, LEE J, STYNER M, CREWS FT. Adolescent binge drinking alters adult brain neurotransmitter gene expression, behavior, brain regional volumes, and neurochemistry in mice. Alcoholism, clinical and experimental research. 2011; 35:671–688.

COLEMAN LG JR, LIU W, OGUZ I, STYNER M, CREWS FT. Adolescent binge ethanol treatment alters adult brain regional volumes, cortical extracellular matrix protein and behavioral flexibility. Pharmacology, biochemistry, and behavior. 2014; 116:142–151.

CREWS F, HE J, HODGE C. Adolescent cortical development: a critical period of vulnerability for addiction. Pharmacology, biochemistry, and behavior. 2007; 86:189–199.

DE BELLIS MD, CLARK DB, BEERS SR, SOLOFF PH, BORING AM, HALL J, KERSH A, KESHAVAN MS. Hippocampal volume in adolescent-onset alcohol use disorders. The American journal of psychiatry. 2000; 157:737–744. [PubMed: 10784466]

DE BELLIS MD, NARASIMHAN A, THATCHER DL, KESHAVAN MS, SOLOFF P, CLARK DB. Prefrontal cortex, thalamus, and cerebellar volumes in adolescents and young adults with adolescent-onset alcohol use disorders and comorbid mental disorders. Alcoholism, clinical and experimental research. 2005; 29:1590–1600.

DEWIT DJ, ADLAF EM, OFFORD DR, OGBORNE AC. Age at first alcohol use: a risk factor for the development of alcohol disorders. The American journal of psychiatry. 2000; 157:745–750. [PubMed: 10784467]

EHLERS CL, OGUZ I, BUDIN F, WILLS DN, CREWS FT. Peri-adolescent ethanol vapor exposure produces reductions in hippocampal volume that are correlated with deficits in prepulse inhibition of the startle. Alcoholism, clinical and experimental research. 2013; 37:1466–1475.

ERNST M, ROMEO RD, ANDERSEN SL. Neurobiology of the development of motivated behaviors in adolescence: a window into a neural systems model. Pharmacology, biochemistry, and behavior. 2009; 93:199–211.

GIEDD JN. Structural magnetic resonance imaging of the adolescent brain. Annals of the New York Academy of Sciences. 2004; 1021:77–85. [PubMed: 15251877]

GIORGIO A, WATKINS KE, DOUAUD G, JAMES AC, JAMES S, DE STEFANO N, MATTHEWS PM, SMITH SM, JOHANSEN-BERG H. Changes in white matter microstructure during adolescence. NeuroImage. 2008; 39:52–61. [PubMed: 17919933]

JACOBUS J, MCQUEENY T, BAVA S, SCHWEINSBURG BC, FRANK LR, YANG TT, TAPERT SF. White matter integrity in adolescents with histories of marijuana use and binge drinking. Neurotoxicology and teratology. 2009; 31:349–355. [PubMed: 19631736]

JOHNSTON, LD.; O'MALLEY, PM.; BACHMAN, JG.; SCHULENBERG, JE. Monitoring the Future National Results on drug use: 2012 Overview, Key Findings on Adolescent Drug Use. Institute for Social Research, The University of Michigan; Ann Arbor: 2013.

JOSHI S, DAVIS B, JOMIER M, GERIG G. Unbiased diffeomorphic atlas construction for computational anatomy. Neuroimage. 2004; 23(Suppl 1):S151–160. [PubMed: 15501084]

JUNG YC, SCHULTE T, MULLER-OEHRING EM, NAMKOONG K, PFEFFERBAUM A, SULLIVAN EV. Compromised frontocerebellar circuitry contributes to nonplanning impulsivity in recovering alcoholics. Psychopharmacology. 2014

KOSKINEN SM, AHVENINEN J, KUJALA T, KAPRIO J, O'DONNELL BF, OSIPOVA D, VIKEN RJ, NAATANEN R, ROSE RJ. A longitudinal twin study of effects of adolescent alcohol abuse on the neurophysiology of attention and orienting. Alcoholism, clinical and experimental research. 2011; 35:1339–1350.

LENROOT RK, GIEDD JN. Brain development in children and adolescents: insights from anatomical magnetic resonance imaging. Neuroscience and biobehavioral reviews. 2006; 30:718–729. [PubMed: 16887188]

LISDAHL KM, THAYER R, SQUEGLIA LM, MCQUEENY TM, TAPERT SF. Recent binge drinking predicts smaller cerebellar volumes in adolescents. Psychiatry research. 2013; 211:17–23. [PubMed: 23154095]

MAC DONALD CL, DIKRANIAN K, BAYLY P, HOLTZMAN D, BRODY D. Diffusion tensor imaging reliably detects experimental traumatic axonal injury and indicates approximate time of injury. The Journal of neuroscience : the official journal of the Society for Neuroscience. 2007; 27:11869–11876. [PubMed: 17978027]

MCQUEENY T, SCHWEINSBURG BC, SCHWEINSBURG AD, JACOBUS J, BAVA S, FRANK LR, TAPERT SF. Altered white matter integrity in adolescent binge drinkers. Alcoholism, clinical and experimental research. 2009; 33:1278–1285.

OGUZ I, LEE J, BUDIN F, RUMPLE A, MCMURRAY M, EHLERS C, CREWS F, JOHNS J, STYNER M. Automatic Skull-stripping of Rat MRI/DTI Scans and Atlas Building. Proceedings - Society of Photo-Optical Instrumentation Engineers. 2011; 7962:7962251–7962257.

OGUZ I, MCMURRAY MS, STYNER M, JOHNS JM. The translational role of diffusion tensor image analysis in animal models of developmental pathologies. Developmental neuroscience. 2012; 34:5–19. [PubMed: 22627095]

OGUZ I, YAXLEY R, BUDIN F, HOOGSTOEL M, LEE J, MALTBIE E, LIU W, CREWS FT. Comparison of magnetic resonance imaging in live vs. post mortem rat brains. PloS one. 2013; 8:e71027. [PubMed: 23967148]

PASCUAL M, BLANCO AM, CAULI O, MINARRO J, GUERRI C. Intermittent ethanol exposure induces inflammatory brain damage and causes long-term behavioural alterations in adolescent rats. The European journal of neuroscience. 2007; 25:541–550. [PubMed: 17284196]

PFEFFERBAUM A, LIM KO, DESMOND JE, SULLIVAN EV. Thinning of the corpus callosum in older alcoholic men: a magnetic resonance imaging study. Alcoholism, clinical and experimental research. 1996; 20:752–757.

ROBERTS TP, SCHWARTZ ES. Principles and implementation of diffusion-weighted and diffusion tensor imaging. Pediatric radiology. 2007; 37:739–748. [PubMed: 17598100]

RUMPLE A, MCMURRAY M, JOHNS J, LAUDER J, MAKAM P, RADCLIFFE M, OGUZ I. 3-dimensional diffusion tensor imaging (DTI) atlas of the rat brain. PloS one. 2013; 8:e67334. [PubMed: 23861758]

SHI Y, SHORT SJ, KNICKMEYER RC, WANG J, COE CL, NIETHAMMER M, GILMORE JH, ZHU H, STYNER MA. Diffusion tensor imaging-based characterization of brain neurodevelopment in primates. Cerebral cortex. 2013; 23:36–48. [PubMed: 22275483]

SNOOK L, PAULSON LA, ROY D, PHILLIPS L, BEAULIEU C. Diffusion tensor imaging of neurodevelopment in children and young adults. NeuroImage. 2005; 26:1164–1173. [PubMed: 15961051]

SONG SK, SUN SW, JU WK, LIN SJ, CROSS AH, NEUFELD AH. Diffusion tensor imaging detects and differentiates axon and myelin degeneration in mouse optic nerve after retinal ischemia. NeuroImage. 2003; 20:1714–1722. [PubMed: 14642481]

SPEAR LP. Rewards, aversions and affect in adolescence: emerging convergences across laboratory animal and human data. Developmental cognitive neuroscience. 2011; 1:392–400. [PubMed: 21918675]

SQUIRE LR. Memory and the hippocampus: a synthesis from findings with rats, monkeys, and humans. Psychological review. 1992; 99:195–231. [PubMed: 1594723]

TAPERT SF, BARATTA MV, ABRANTES AM, BROWN SA. Attention dysfunction predicts substance involvement in community youths. Journal of the American Academy of Child and Adolescent Psychiatry. 2002; 41:680–686. [PubMed: 12049442]

THISSEN D, STEINBERG L, KUANG D. Quick and easy implementation of the Benjamini-Hochberg procedure for controlling the false positive rate in multiple comparisons. Journal of Educational and Behavioral Statistics. 2002; 27:77–83.

VETRENO RP, CREWS FT. Adolescent binge drinking increases expression of the danger signal receptor agonist HMGB1 and Toll-like receptors in the adult prefrontal cortex. Neuroscience. 2012; 226:475–488. [PubMed: 22986167]

WANG Y, ADAMSON C, YUAN W, ALTAYE M, RAJAGOPAL A, BYARS AW, HOLLAND SK. Sex differences in white matter development during adolescence: a DTI study. Brain research. 2012; 1478:1–15. [PubMed: 22954903]

WELCH KA, CARSON A, LAWRIE SM. Brain structure in adolescents and young adults with alcohol problems: systematic review of imaging studies. Alcohol and alcoholism. 2013; 48:433–444. [PubMed: 23632805]

WHITE AM, KRAUS CL, SWARTZWELDER H. Many college freshmen drink at levels far beyond the binge threshold. Alcoholism, clinical and experimental research. 2006; 30:1006–1010.

WHITE HR, MARMORSTEIN NR, CREWS FT, BATES ME, MUN EY, LOEBER R. Associations between heavy drinking and changes in impulsive behavior among adolescent boys. Alcoholism, clinical and experimental research. 2011; 35:295–303.

WRIGHT JW, MASINO AJ, REICHERT JR, TURNER GD, MEIGHAN SE, MEIGHAN PC, HARDING JW. Ethanol-induced impairment of spatial memory and brain matrix metalloproteinases. Brain research. 2003; 963:252–261. [PubMed: 12560131]

WU M, LU LH, LOWES A, YANG S, PASSAROTTI AM, ZHOU XJ, PAVULURI MN. Development of superficial white matter and its structural interplay with cortical gray matter in children and adolescents. Human brain mapping. 2014; 35:2806–2816. [PubMed: 24038932]

ZHANG J, AGGARWAL M, MORI S. Structural insights into the rodent CNS via diffusion tensor imaging. Trends in neurosciences. 2012; 35:412–421. [PubMed: 22651954]

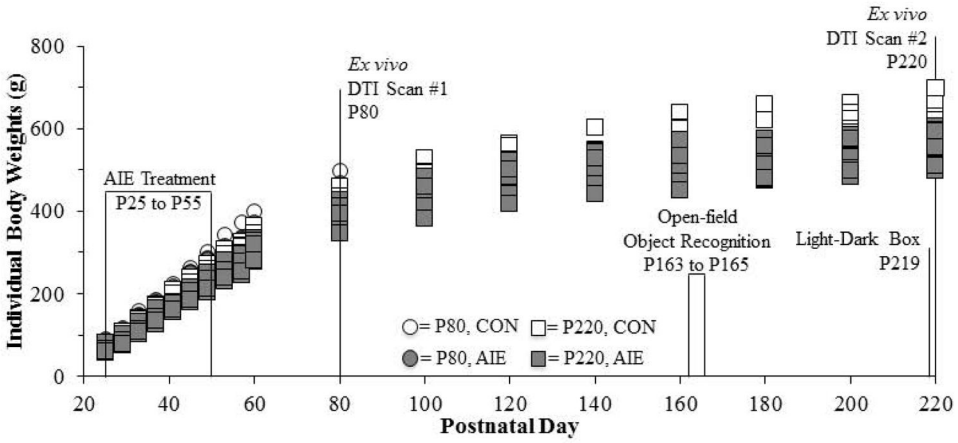

Figure 1. Graphical representation of the adolescent intermittent ethanol (AIE) treatment paradigm

Rats received either ethanol (5.0 g/kg, 20% ethanol w/v, i.g.) or a comparable volume of water from postnatal day (P)25 to P55 on a 2-day on/2-day off administration schedule. Blood ethanol concentrations (BECs) were assessed one hr after ethanol exposure on P38 and P54. Subjects in the first age group were sacrificed on P80 for diffusion tensor imaging (DTI) analysis. Subjects in the second age group were behaviorally tested on the open-field object recognition task from P163 to P165 and on the light/dark box anxiety test on P219. The subjects were then sacrificed on P220 for DTI analysis.

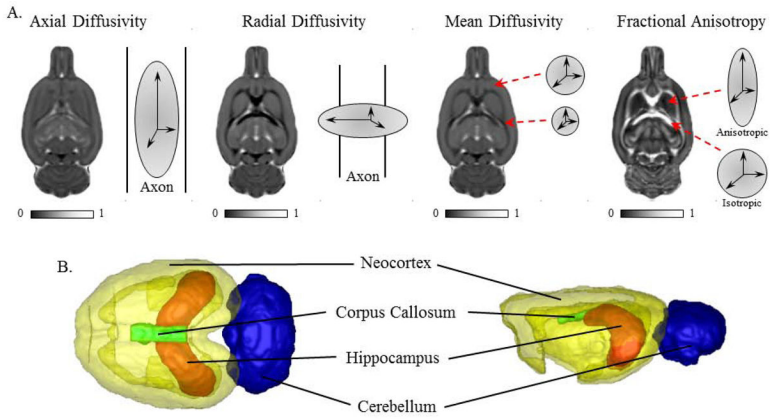

Figure 2. Diffusion tensor imaging (DTI) schematics

(A) Representative scans depicting axial diffusivity, radial diffusivity, mean diffusivity, and fractional anisotropy from a CON subject in the postnatal (P)220 age group. Axial diffusivity provides a measure of the magnitude and directionality of water movement parallel to the axon. It allows for inferences of axonal integrity, and/or cellular organization (Zhang et al., 2012), with higher values indicative of increased axonal integrity. Radial diffusivity provides a measure of the magnitude of water diffusion perpendicular to the axon, and decreased values are associated with to increased tissue density (Giorgio et al., 2008; Snook et al., 2005). Mean diffusivity is an overall indication of the magnitude of the diffusion of water and allows for inferences regarding cellular size and integrity (Cercignani et al., 2001). Lower mean diffusivity values are associated with increased tissue density (Roberts and Schwartz, 2007). Fractional anisotropy provides the degree of directionally-dependent water diffusion and is related to axonal density and/or myelination (Beaulieu, 2002). (B) Schematic depicting neocortex, corpus callosum, hippocampus, and cerebellum from a CON subject in the P220 age group.

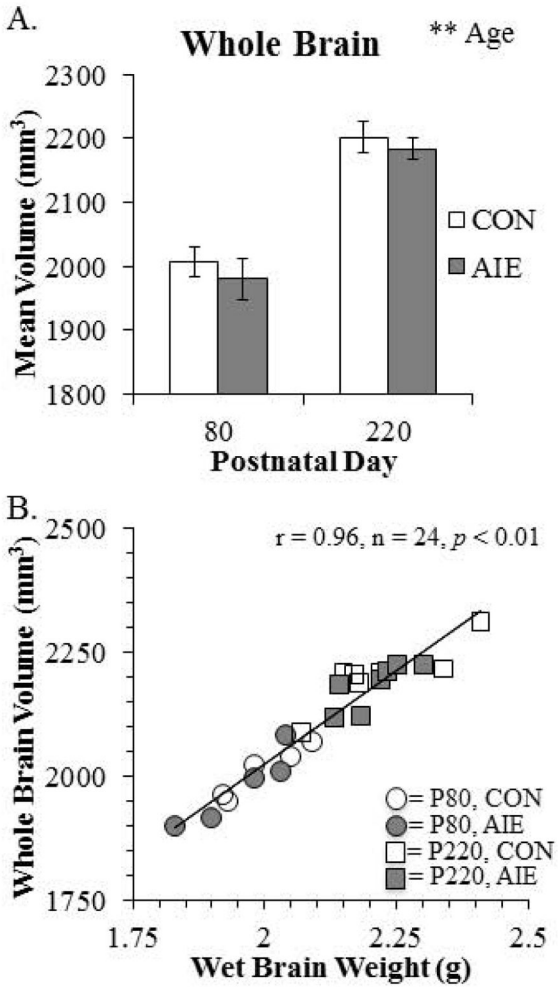

Figure 3. Diffusion tensor imaging (DTI) reveals that whole brain volumes increase from postnatal day (P)80 to P220 and correlate with wet brain weight

(A) DTI analysis revealed that whole brain volume (mm^3) increased from P80 to P220 (main effect of AGE: $F_{(1,20)} = 65.6$, $p < 0.01$) that did not interact with adolescent intermittent ethanol (AIE) treatment. **, $p < 0.01$. (B) Pearson's r correlation found that whole brain volumes (mm^3) were positively correlated with wet brain weights (g; r = 0.96, n = 24, $p < 0.01$).

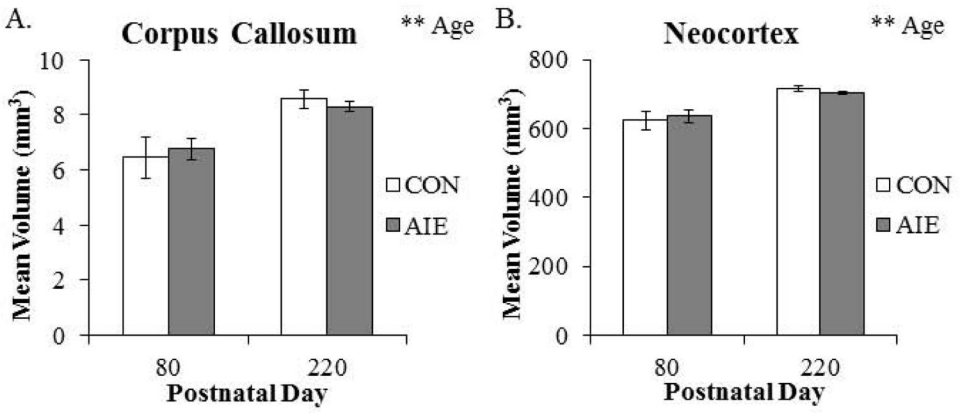

Figure 4. Volumes of corpus callosal white matter and neocortical grey matter increase from postnatal day (P)80 to P220

Diffusion tensor imaging revealed that (A) corpus callosum volume (main effect of AGE: $F_{(1,20)} = 20.3$, $p < 0.01$) and (B) neocortex volume (main effect of AGE: $F_{(1,20)} = 31.7$, $p < 0.01$) continued to increase from P80 to P220. Adolescent intermittent ethanol (AIE) treatment did not affect brain regional volumes at these ages. Depicted are means ± S.E.M. **, $p < 0.01$.

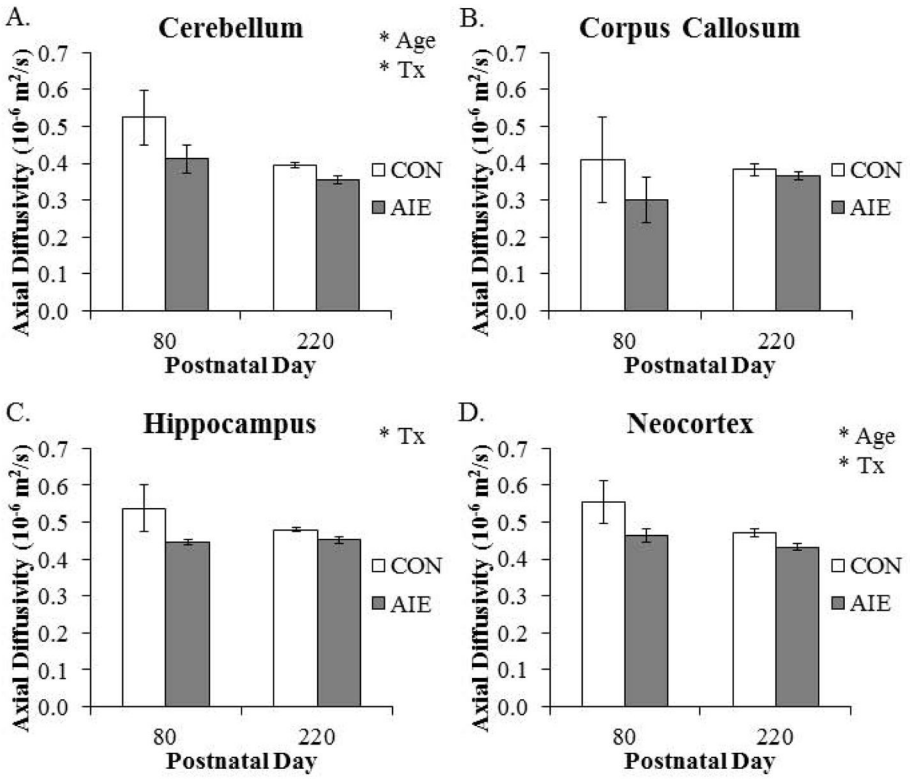

Figure 5. Adolescent intermittent ethanol (AIE) exposure and aging lead to brain regional specific alterations of axial diffusivity (AD) in the adult brain

(A) Within the cerebellum, AD declined from postnatal day (P)80 to P220 (main effect of AGE: $F_{(1,20)} = 6.9$, $p < 0.05$), and was significantly reduced in the AIE-treated animals, relative to the CONs (main effect of TREATMENT: $F_{(1,20)} = 4.4$, $p < 0.05$). (B) Corpus callosum AD was unaffected by aging or AIE treatment. (C) Axial diffusivity was significantly decreased in the hippocampus of AIE-treated animals, relative to CONs (main effect of TREATMENT: $F_{(1,20)} = 4.8$, $p < 0.05$). (D) Neocortical AD declined from P80 to P220 (main effect of AGE: $F_{(1,20)} = 4.9$, $p < 0.05$, and was significantly decreased by AIE treatment (main effect of TREATMENT: $F_{(1,20)} = 6.2$, $p < 0.05$). Depicted are means ±S.E.M. * $p < 0.05$.

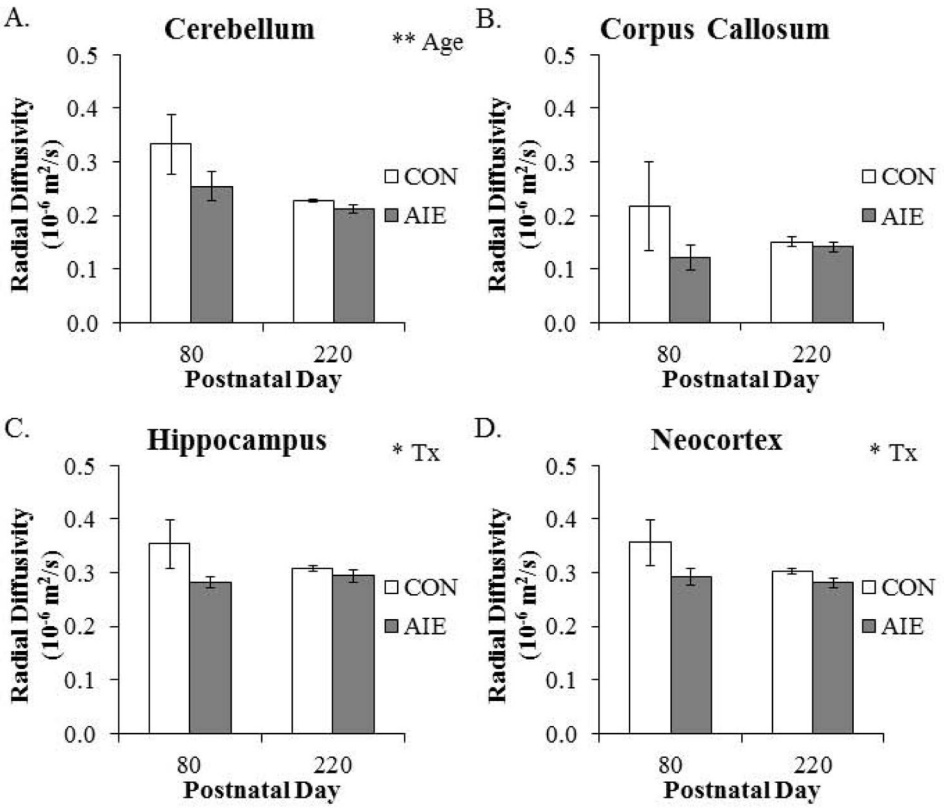

Figure 6. Radial diffusivity (RD) is altered across aging and by adolescent intermittent ethanol (AIE) treatment in the adult brain

(A) Radial diffusivity in the cerebellum declined from postnatal day (P)80 to P220 (main effect of AGE: $F_{(1,20)} = 8.0$, $p = 0.01$). (B) Corpus callosal RD was unaffected by aging or AIE treatment. (C) Within the hippocampus, RD was significantly reduced in the AIE-treated animals, relative to the CONs (main effect of TREATMENT: $F_{(1,20)} = 4.2$, $p = 0.05$). (D) There was a significant AIE-induced decrease of RD in the neocortex, relative to CONs (main effect of TREATMENT: $F_{(1,20)} = 4.5$, $p < 0.05$). Depicted are means ± S.E.M. * $p < 0.05$, ** $p \leq 0.01$.

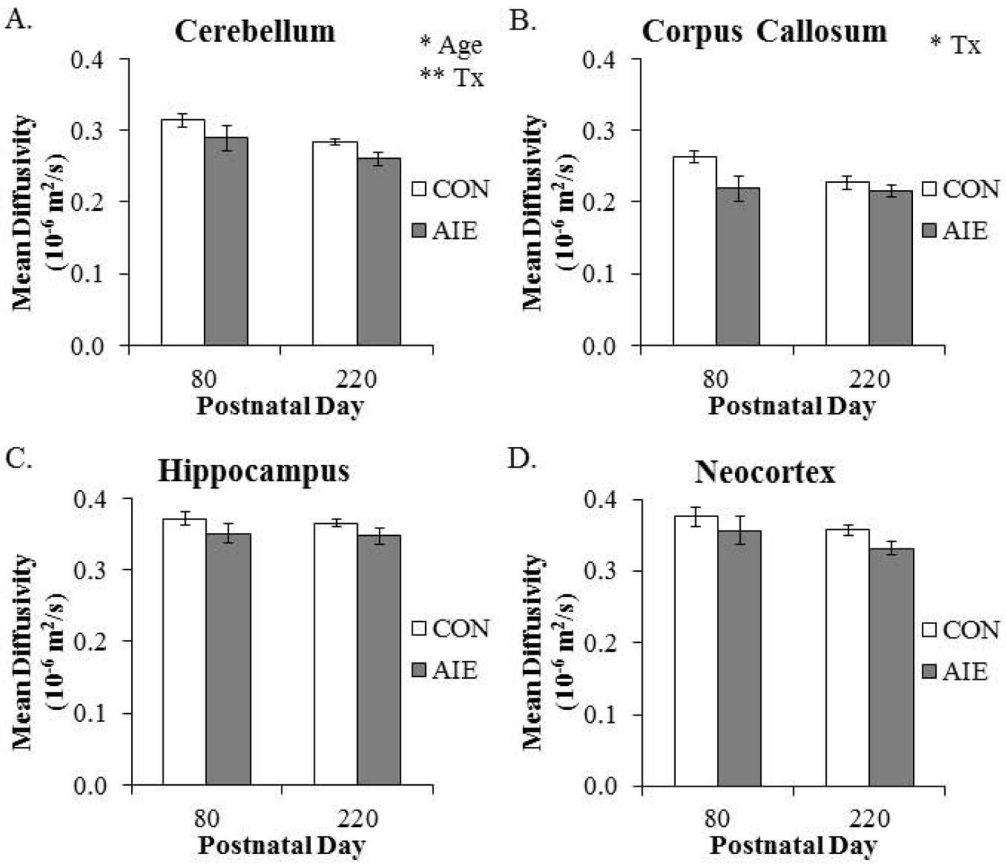

Figure 7. Diffusion tensor imaging reveals that aging and adolescent intermittent ethanol (AIE) affect mean diffusivity (MD) in the adult brain

(A) Cerebellar MD declined from postnatal day (P)80 to P220 (main effect of AGE: $F_{(1,20)} = 5.8$, $p < 0.05$), and was significantly decreased by AIE treatment, relative to CONs (main effect of TREATMENT: $F_{(1,20)} = 8.6$, $p < 0.01$). (B) Adolescent intermittent ethanol treatment significantly reduced MD in the corpus callosum, relative to CONs (main effect of TREATMENT: $F_{(1,20)} = 6.1$, $p < 0.05$). (C) Hippocampal MD was unaffected by aging or AIE treatment. (D) Neocortex AD was unaffected by aging or AIE treatment. Depicted are means ± S.E.M. * $p < 0.05$, ** $p < 0.01$.

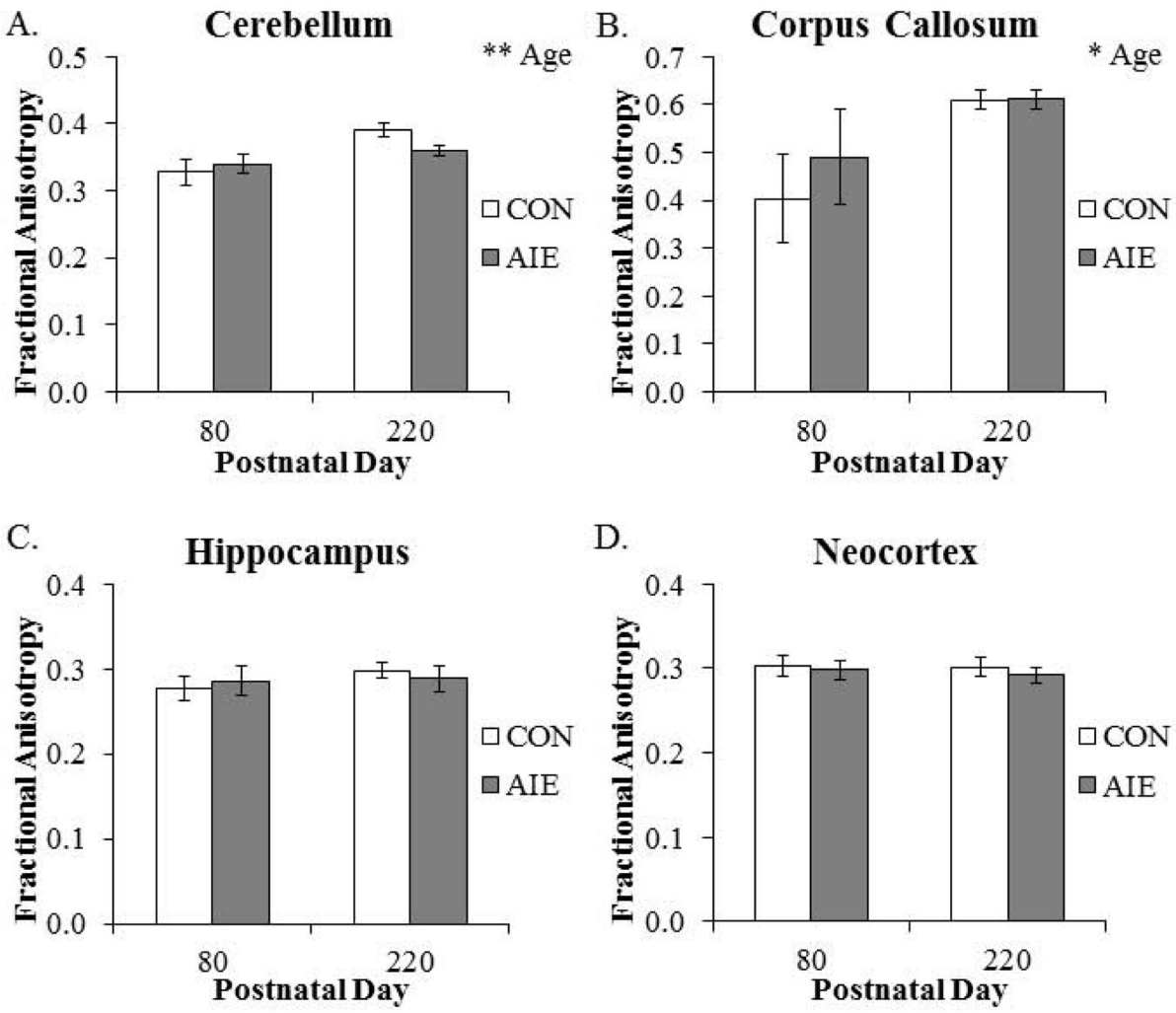

Figure 8. Diffusion tensor imaging reveals that factional anisotropy is increased in both grey and white matter structures across aging

Fractional anisotropy was significantly increased in the (A) cerebellum (main effect of AGE: $F_{(1,20)} = 10.4$, $p < 0.01$) and (B) corpus callosum (main effect of AGE: $F_{(1,20)} = 7.6$, $p < 0.05$) from postnatal day (P)80 to P220. (C) Hippocampal FA was unaffected by aging or AIE treatment. (D) Neocortex FA was unaffected by aging or AIE treatment. Adolescent intermittent ethanol (AIE) treatment did not affect brain regional volumes at these ages. Depicted are means ± S.E.M. *, $p < 0.05$, ** $p < 0.01$.

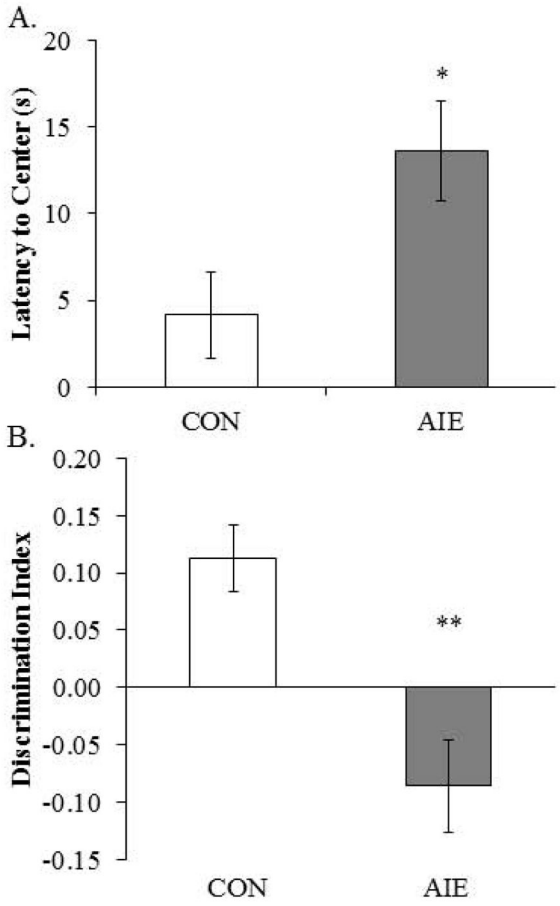

Figure 9. Adolescent intermittent ethanol (AIE) treatment leads to long-term deficits in object recognition memory

(A) Latency to enter the center of the open-field apparatus during the first trial, which provides a measure of thigmotaxis, was significantly increased in adult rats following AIE treatment (one-way ANOVA: $F_{(1,13)} = 6.3$, $p < 0.05$). (B) Adolescent intermittent ethanol treatment significantly reduced the discrimination index, which is indicative of impaired object recognition memory, in adult rats relative to CONs (one-way ANOVA: $F_{(1,13)} = 16.3$, $p < 0.01$). Depicted are means ± S.E.M. * $p < 0.05$, ** $p < 0.01$.

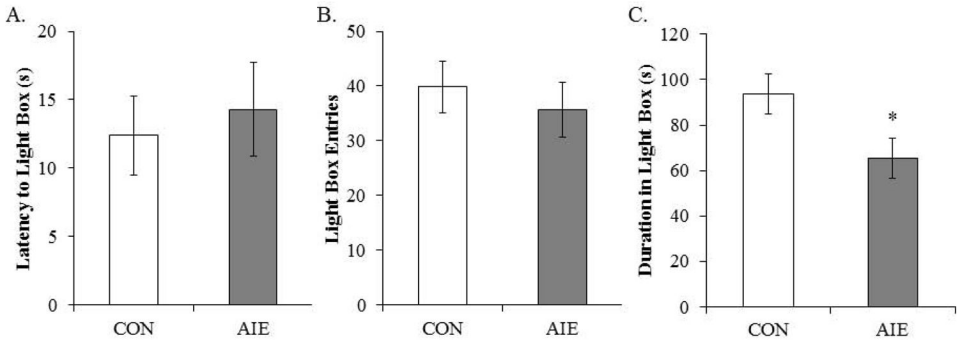

Figure 10. Adolescent intermittent ethanol (AIE) treatment leads to long-term alterations in light/dark box behavior

Neither the latency to enter the light box (A) nor light box entries (B) was affected in adulthood by prior AIE treatment. However, duration in the light box (C) was significantly reduced by AIE treatment in adulthood, relative to CONs (one-way ANOVA: $F_{(1,13)} = 6.1$, $p < 0.05$). Depicted are means ± S.E.M. *, $p < 0.05$.

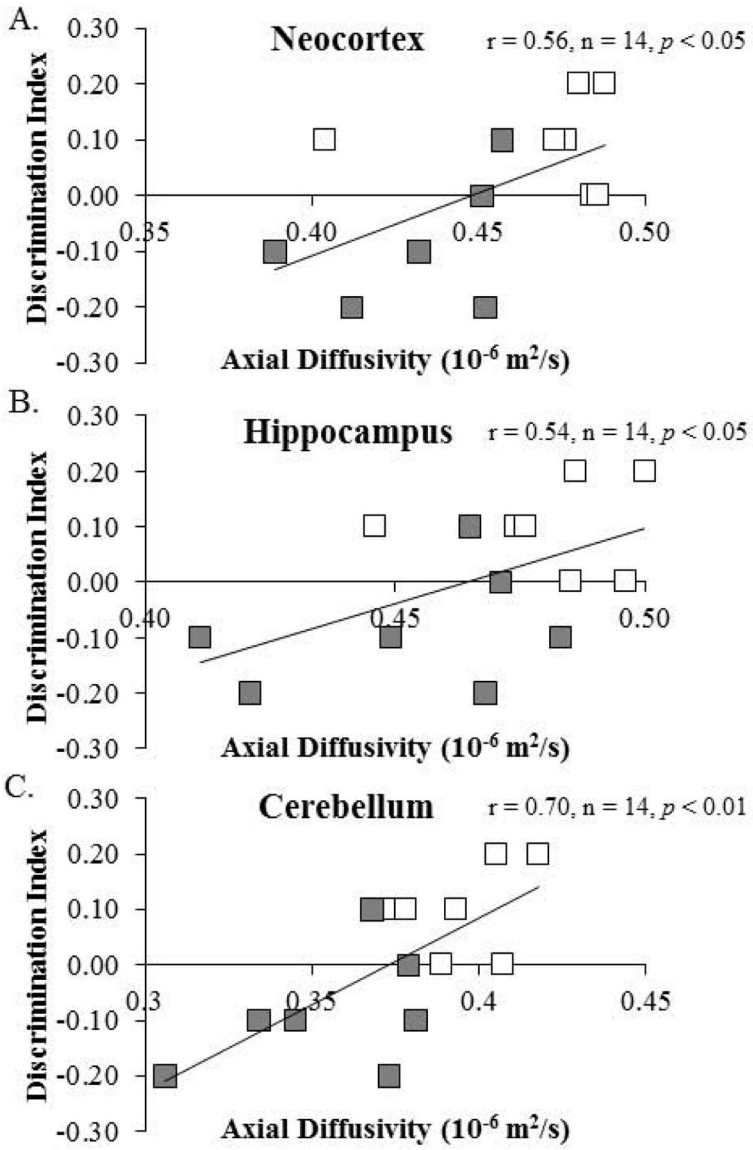

Figure 11. Axial diffusivity (AD) in the neocortex, hippocampus, and cerebellum is correlated with object recognition memory performance in adulthood

Performance on the open-field object recognition memory test is positively correlated AD measures in the (A) neocortex (r = 0.56, n = 14, $p < 0.05$), (B) hippocampus (r = 0.54, n = 14, $p < 0.05$), and (C) cerebellum (r = 0.70, n = 14, $p < 0.01$).

Table 1

Diffusion tensor imaging (DTI) analysis of brain regional volumes across treatment at different ages.

Volume (mm^3)									
Postnatal Day 80					Postnatal Day 220				
Structure	**CON**	**AIE**	***p*-value**	**B-H Critical**	**Structure**	**CON**	**AIE**	***p*-value**	**B-H Critical**
Amygdala	21.06	20.60	0.903	0.025	Amygdala	20.23	19.49	0.281	0.014
Cerebellum	295.18	280.52	0.722	0.021	Cerebellum	284.17	287.96	***0.020***	0.004
Corpus Callosum	6.45	6.76	0.714	0.018	Corpus Callosum	8.59	8.29	0.641	0.025
Hippocampus	100.49	93.68	0.707	0.014	Hippocampus	102.43	99.92	0.265	0.011
Hypothalamus	66.22	62.50	0.705	0.011	Hypothalamus	65.73	60.95	0.389	0.018
Neocortex	624.19	636.68	0.535	0.007	Neocortex	716.67	705.21	***0.045***	0.007
Striatum	88.21	81.10	0.530	0.004	Striatum	82.60	88.44	0.483	0.021

The effect of adolescent intermittent ethanol (AIE) treatment on select adult brain regional volumes using DTI at postnatal day (P)80 and P220. Volumes of the individual structures (mm^3) in CON and AIE groups (mean), the *p* value (t-test), and Benjamini-Hochberg procedure (B-H Critical) for controlling false positives are shown. A particular t-test is significant based on the B-H Critical if the *p* value is less than the B-H Critical value. Although the cerebellum and neocortex in the P220 age group differ based on t-tests (***bold***), they did not meet the B-H critical criteria for false positive control.

Addict Biol. Author manuscript; available in PMC 2017 July 01.

Table 2

Diffusion tensor imaging (DTI) analysis of axial diffusivity (AD) across treatment at different ages.

Axial Diffusivity (10^{-6} mm^2/s)									
Postnatal Day 80					**Postnatal Day 220**				
Structure	**CON**	**AIE**	***p*-value**	**B-H Critical**	**Structure**	**CON**	**AIE**	***p*-value**	**B-H Critical**
Amygdala	0.559	0.472	0.361	0.018	Amygdala	0.437	0.410	0.271	0.018
Cerebellum	0.524	0.413	0.226	0.014	Cerebellum	0.395	0.355	***0.007***	0.004
Corpus Callosum	0.409	0.301	0.438	0.025	Corpus Callosum	0.383	0.366	0.387	0.021
Hippocampus	0.537	0.446	0.189	0.011	Hippocampus	0.480	0.452	***0.042***	0.011
Hypothalamus	0.526	0.443	0.423	0.021	Hypothalamus	0.368	0.341	0.153	0.014
Neocortex	0.555	0.463	0.160	0.004	Neocortex	0.470	0.432	***0.023***	0.007
Striatum	0.524	0.410	0.180	0.007	Striatum	0.398	0.399	0.968	0.025

The effect of adolescent intermittent ethanol (AIE) treatment on select adult brain regional AD values using DTI at postnatal day (P)80 and P220. Axial diffusivity of the individual structures (10^{-6} mm^2/s) in CON and AIE groups (mean), the *p* value (t-test), and Benjamini-Hochberg procedure (B-H Critical) for controlling false positives are shown. A particular t-test is significant based on the B-H Critical if the *p* value is less than the B-H Critical value. Although the cerebellum, hippocampus, and neocortex in the P220 age group differ based on individual t-tests (***bold***), they did not meet the B-H critical criteria for false positive control.

Table 3

Diffusion tensor imaging analysis of radial diffusivity (RD) across treatment at different ages.

Radial Diffusivity (10^{-6} mm^2/s)									
Postnatal Day 80					Postnatal Day 220				
Structure	**CON**	**AIE**	***p*-value**	**B-H Critical**	**Structure**	**CON**	**AIE**	***p*-value**	**B-H Critical**
Amygdala	0.358	0.300	0.397	0.021	Amygdala	0.264	0.250	0.279	0.014
Cerebellum	0.333	0.254	0.232	0.014	Cerebellum	0.228	0.212	0.092	0.004
Corpus Callosum	0.218	0.121	0.292	0.018	Corpus Callosum	0.150	0.141	0.471	0.021
Hippocampus	0.354	0.283	0.161	0.007	Hippocampus	0.308	0.294	0.328	0.018
Hypothalamus	0.330	0.277	0.476	0.025	Hypothalamus	0.209	0.186	0.172	0.011
Neocortex	0.356	0.293	0.199	0.011	Neocortex	0.303	0.282	0.092	0.007
Striatum	0.355	0.276	0.145	0.004	Striatum	0.275	0.277	0.831	0.025

The effect of adolescent intermittent ethanol (AIE) treatment on select adult brain regional RD values using DTI at postnatal day (P)80 and P220. Radial diffusivity of the individual structures (10^{-6} mm^2/s) in CON and AIE groups (mean), the *p* value (t-test), and Benjamini-Hochberg procedure (B-H Critical) for controlling false positives are shown. A particular t-test is significant based on the B-H Critical if the *p* value is less than the B-H Critical value. None of the individual t-tests revealed a significant effect of AIE treatment at either age.

Table 4

Diffusion tensor imaging (DTI) analysis of mean diffusivity (MD) across treatment at different ages.

Mean Diffusivity (10^{-6} mm^2/s)									
Postnatal Day 80					Postnatal Day 220				
Structure	**CON**	**AIE**	***p*-value**	**B-H Critical**	**Structure**	**CON**	**AIE**	***p*-value**	**B-H Critical**
Amygdala	0.340	0.327	0.457	0.021	Amygdala	0.322	0.304	0.243	0.018
Cerebellum	0.314	0.289	0.243	0.011	Cerebellum	0.284	0.260	***0.031***	0.004
Corpus Callosum	0.263	0.219	0.055	0.004	Corpus Callosum	0.227	0.216	0.386	0.021
Hippocampus	0.371	0.351	0.282	0.014	Hippocampus	0.365	0.347	0.158	0.014
Hypothalamus	0.304	0.295	0.670	0.025	Hypothalamus	0.262	0.238	0.135	0.011
Neocortex	0.376	0.357	0.439	0.018	Neocortex	0.358	0.332	***0.043***	0.007
Striatum	0.335	0.320	0.217	0.007	Striatum	0.316	0.317	0.845	0.025

The effect of adolescent intermittent ethanol (AIE) treatment on select adult brain regional MD values using DTI at postnatal day (P)80 and P220. Mean diffusivity of the individual structures (10^{-6} mm^2/s) in CON and AIE groups (mean), the *p* value (t-test), and Benjamini-Hochberg procedure (B-H Critical) for controlling false positives are shown. A particular t-test is significant based on the B-H Critical if the *p* value is less than the B-H Critical value. While the cerebellum and neocortex in the P220 age group differ based on individual t-tests (***bold***), they did not meet the B-H critical criteria for false positive control.

Table 5

Diffusion tensor imaging (DTI) analysis of fractional anisotropy (FA) across treatment at different ages.

Fractional Anisotropy									
Postnatal Day 80					Postnatal Day 220				
Structure	**CON**	**AIE**	***p*-value**	**B-H Critical**	**Structure**	**CON**	**AIE**	***p*-value**	**B-H Critical**
Amygdala	0.316	0.315	0.964	0.025	Amygdala	0.337	0.331	0.743	0.014
Cerebellum	0.328	0.340	0.651	0.011	Cerebellum	0.391	0.360	***0.042***	0.004
Corpus Callosum	0.404	0.490	0.551	0.004	Corpus Callosum	0.610	0.611	0.977	0.025
Hippocampus	0.277	0.286	0.700	0.014	Hippocampus	0.298	0.289	0.613	0.011
Hypothalamus	0.324	0.322	0.944	0.021	Hypothalamus	0.381	0.391	0.786	0.018
Neocortex	0.303	0.298	0.764	0.018	Neocortex	0.302	0.292	0.508	0.007
Striatum	0.271	0.259	0.563	0.007	Striatum	0.256	0.250	0.787	0.021

The effect of adolescent intermittent ethanol (AIE) treatment on select adult brain regional FA values using DTI at postnatal day (P)80 and P220. Fractional anisotropy of the individual structures in CON and AIE groups (mean), the *p* value (t-test), and Benjamini-Hochberg procedure (B-H Critical) for controlling false positives are shown. A particular t-test is significant based on the B-H Critical if the *p* value is less than the B-H Critical value. Although FA in the cerebellum of the P220 age group differed based on an individual t-test (***bold***), it did not meet the B-H critical criteria for false positive control.

Table 6

Correlations of diffusion tensor imaging measures in the adult brain with object recognition memory.

Structure	AD	RD	MD	FA
Amygdala	0.39	0.39	0.41	0.06
Cerebellum	0.70**	0.54*	0.63*	0.34
Corpus Callosum	0.48	0.33	0.43	−0.04
Hippocampus	0.54*	0.37	0.45	−0.02
Hypothalamus	0.43	0.47	0.49	−0.21
Neocortex	0.56*	0.53*	0.57*	−0.01
Striatum	0.06	0.20	0.16	−0.08

Pearson's r correlations were conducted for the seven regions of interest with behavioral performance on the open-field object recognition task. Although our correlations do not prove definitive conclusions, we found statistically significant associations between object recognition memory and diffusivity measures in the cerebellum, hippocampus, and neocortex. AD: axial diffusivity; RD: radial diffusivity; MD: mean diffusivity; FA: fractional anisotropy.

*Pearson's r correlation coefficients were used with two-tailed significance ($p < 0.05$).

**Pearson's r correlation coefficients were used with two-tailed significance ($p < 0.01$).